Published in final edited form as:
Clin Lab Med. 2007 September ; 27(3): 653–viii.

Cellular Image Analysis and Imaging by Flow Cytometry

David A. Basiji, PhD, **William E. Ortyn**, **Luchuan Liang, PhD**, **Vidya Venkatachalam, PhD**, and **Philip Morrissey, PhD**
Amnis Corporation, Seattle, Washington

Synopsis

Imaging flow cytometry combines the statistical power and fluorescence sensitivity of standard flow cytometry with the spatial resolution and quantitative morphology of digital microscopy. The technique is a good fit for clinical applications by providing a convenient means for imaging and analyzing cells directly in bodily fluids. Examples are provided of the discrimination of cancerous from normal mammary epithelial cells and the high throughput quantitation of FISH probes in human peripheral blood mononuclear cells. The FISH application will be further enhanced by the integration of extended depth of field imaging technology with the current optical system.

Keywords

imaging; flow; cytometry; fluorescence; brightfield; darkfield; multispectral

Quantifying Cellular Structure in Health and Disease

The eukaryotic cell is a highly structured, three-dimensional object containing a wide range of molecular species. The size, shape, and structure of the cell, as well as the abundance, location, and co-location of any of these constituent biomolecules may be of significance in any given clinical situation or research application. For instance, in hematopoiesis, as cells differentiate and mature, different subsets of molecules are expressed that reflect a specialized functional capacity for that unique cell type (e.g., granulocytes vs. lymphocytes). In general the characterization of this array of constituent molecules by imaging or flow cytometry provides insight into the physiological function of any particular cell or alternatively, pathological changes that may have occurred or accrued. In clinical practice and in research settings, cellular evaluation by imaging technologies and flow cytometry provides significant information reflecting the particular cellular phenotype, both normal and pathological. Microscopy provides a wealth of information, but data acquisition rates are slow and analysis is generally subjective. In flow cytometry, data acquisition is rapid and better suited for the evaluation of pathologies present in low frequency, but the data are only intensity-based, thus lacking the morphology that truly lends credence to the analysis.

In addition, the assessment and evaluation of cell samples by imaging and flow cytometric techniques is complicated by a number of factors. For instance, changes in a cell type or

aCorresponding author for proofs and reprints: David A. Basiji, PhD, Amnis Corporation, 2505 Third Ave., Suite 210, Seattle, WA 98121, (206) 374-7165, (206) 576-6895 (fax), dbasiji@amnis.com (email)

Disclosure: The authors of this chapter are shareholders and in the employ of Amnis Corporation. This work was partially supported by grant numbers 9 R44 CA01798-02 and 1 R43 GM58956-01 from the National Institutes of Health and contract number NNA05CR09C from the National Aeronautics and Space Administration.

phenotypic changes in a cell subpopulation often occur in heterogeneous cell mixtures; there is phenotypic variability amongst populations, especially in human clinical settings; and the cell population of interest may be present in a very low frequency. The relative benefits of technologies to evaluate cells and cell populations will be discussed in this context.

Comparisons of Technologies

Every form of cytologic instrumentation represents a compromise. As a general rule, there's a tradeoff between acquisition speed, fluorescence sensitivity, and information content. For example, a confocal microscope can produce highly detailed fluorescent cell images, including three dimensional cell representations based on multiple stacked images, but it can take as long as several minutes to produce a high resolution 3D representation of a single cell. Absolute fluorescence sensitivity is also generally lower in confocal microscopy than other techniques because out-of-focus signals are rejected by the confocal optical system and because the image is built up serially from individual measurements at every location across the cell, reducing the amount of time available to collect signal. Sensitivity may be increased in a single image by dwelling over the cell for a longer period of time, but this can cause excessive photobleaching outside of the plane of focus, hindering 3D imaging. The design features associated with confocal microscopy make it well-suited to applications that require the accurate analysis of sub-cellular features in homogeneous samples, but poorly suited to detecting faint fluorescent probes or evaluating statistically significant numbers of cells within heterogeneous samples. Although high resolution, 3D representations of cells by confocal imaging may be useful in certain areas of clinical research, confocal imaging is not widely used in clinical assessment or diagnostics.[1, 2]

At the opposite functional extreme from confocal microscopy is flow cytometry. The most obvious difference between the techniques is that flow cytometry requires cells to be in suspension rather than on slides. Further, flow cytometry sacrifices imaging entirely in favor of high acquisition rates and fluorescence sensitivity. In flow cytometry, each detection event (cell) is associated with several numerical measurements of fluorescence intensity and the degree of forward and side scatter of laser light. Forward scatter is roughly correlated to the size of the cell and side scatter gives an indication of the cell's granularity, but flow cytometry offers no means of sub-cellular fluorescence localization. The strength of flow cytometry is that it allows the rapid analysis of large populations of cells. Typical analytical throughput is 5,000 cells per second, which means that even rare cell populations (i.e. less than 1 cell in 10,000) can be detected in statistically significant numbers in a reasonable period of time. Fluorescence detection limits are often less than 100 molecules per cell. The combination of high speed and high quantitative fluorescence sensitivity makes the technique well-suited, for situations such as ectopic expression of ZAP-70 in CLL, which is a prognostic indicator.[3]

The third example of cellular analysis techniques is standard microscopy. In contrast to confocal microscopy, standard microscopy can image cells in a variety of modes (transmitted light, scattered light, fluorescence, phase contrast, etc.), each of which provides distinct and complementary information about the cell. For a given imaging rate, fluorescence sensitivity is generally better than confocal microscopy and given sufficient time to integrate signal, sensitivity can even exceed flow cytometry. In automated form, standard microscopy can be both quantitative and relatively fast, with a typical throughput of several hundred cells per second. Though the spatial resolution of standard microscopy is not as good as confocal microscopy, it is sufficient to resolve many sub-cellular compartments and structures, making it the standard of practice for clinical cytologic evaluations.

Partly as a result of the constraints imposed by their instrumentation, many clinicians employ expert, but subjective, assessment of a few hundred cell images via standard microscopy,

combined with a separate flow cytometric analysis for the quantitative assessment of cellular phenotype and cell cycle. This means that the sample must be split and processed using two distinct protocols. If the primary cell sample is in suspension, (e.g., blood, lavages, etc.), it is straightforward to prepare it for flow cytometry, but for microscopic assessment the cell sample must be smeared, cytospun, or otherwise adhered on a slide or solid substrate prior to staining and visual examination, with the associated risks of staining variability or altered cell morphology. Conversely, with primary solid tissue samples the preparation of a slide for microscopic assessment is relatively simple, but for flow cytometry the sample must be disaggregated prior to staining and data acquisition. Thus, the clinician is forced to use a mix of highly informative image data from relatively few cells and highly quantitative but limited data from statistically meaningful cell populations, often taken at different times and/or subject to different preparation and data acquisition biases.

Ideally, the clinician would employ a single sample preparation protocol and have access to imagery from as many cells as needed in order to provide a robust quantitative analysis of cellular features suggesting a limited number of possible diagnoses. For cells in bodily fluids those that are in suspension by virtue of the sampling technique (e.g., fine needle biopsy), high speed digital imaging of cells in flow coupled with software capable of quantitative image analysis on large numbers of cells, makes it possible to achieve this goal.

Imaging Flow Cytometry

A number of techniques have been developed for imaging cells in flow, starting very shortly after the advent of conventional flow cytometry. Approaches have included strobed illumination techniques, flying spot scanning, mirror tracking, and slit scanning flow cytometry.[4, 5] The challenges associated with imaging cells in flow include achieving sufficient fluorescence sensitivity, producing imagery with high spatial resolution, combining fluorescence imagery with other imaging modes such as brightfield (transmitted light) or darkfield (scattered light), and imaging all of the cells in the flow stream. Until recently, no technique has been able to combine all of these traits but advances over the last 10 years in CCD camera technology, optical filtration, and digital computing have now made it practical.

The ImageStream® system is a commercially available imaging flow cytometer that takes advantage of these advances in technology. The system combines a precise method of electronically tracking moving cells with a high resolution multispectral imaging system to acquire multiple images of each cell in different imaging modes. The current commercial embodiment simultaneously acquires six images of each cell, with fluorescence sensitivity comparable to conventional flow cytometry and the image quality of 40X-60X microscopy.[6, 7] The six images of each cell comprise: a side-scatter (darkfield) image, a transmitted light (brightfield) image, and four fluorescence images corresponding roughly to the FL1, FL2, FL3, and FL4 spectral bands of a conventional flow cytometer. The imaging objective has a numeric aperture of 0.75 and image quality is comparable to 40X to 60X microscopy, as judged by eye. With a throughput up to 300 cells per second, this system can produce 60,000 images of 10,000 cells in about 30 seconds and 600,000 images of 100,000 cells in just over 5 minutes.

The development of reliable hardware to acquire tens of thousands of images requires flexible and powerful analytical software to distill the most appropriate cellular features from the data, including quantitative morphology, fluorescent signal strength, signal locations, and other image characteristics for any particular indication. The ImageStream system utilizes the IDEAS® data analysis software package that currently calculates over 40 quantitative features per image, resulting in approximately 250 features per cell. These features can be used by the clinician or researcher to generate histograms and scatter plots much like a standard flow cytometry data analysis programs, though the various image-based features allow the graphical

identification of populations based not only on fluorescence intensity, but also cell size, shape, texture, probe distribution heterogeneity, co-localization of multiple probes, etc. Once the populations of interest have been identified, they can be visually inspected and characterized by their associated feature values using population statistics, including means, medians, standard deviations, and standard statistical tests. A sufficiently large population will give rise to a relatively narrow standard deviation and allow the detection of subtle differences between samples based on changes in the population's mean feature values.

Detection and Discrimination of Tumor Cells

Carcinomas are the most common form of cancer and are responsible for the majority of cancer-related deaths worldwide.[8] Early detection of cancer significantly improves the prognosis, as evidenced by the 70% reduction in mortality in cervical cancer after the Pap smear became accepted as a routine annual examination in the United States.[9] Likewise, mortality rates from breast cancer are reduced up to 30% due to earlier detection through manual examination or mammography.[10] Unfortunately, the inaccessibility of most body tissues currently limits the breadth of cancer screening. Even when tumors are detected by existing means and removed surgically, there is a strong inverse correlation between tumor size and outcome, as the prior dissemination of metastatic cells often leads to mortality.[11, 12]

The analysis of accessible body fluids for the detection of neoplastic cells would greatly facilitate earlier cancer detection, while the detection of micrometastases in body fluids of patients with early stage cancer could have a substantial impact on optimizing therapeutic regimens and thus, long term prognosis. Imaging flow cytometry has the potential to increase the early detection of certain cancers via the analysis of cells in bodily fluids, such as detection of bladder cancer via the urine and lung cancer via sputum.

Detecting neoplastic epithelial cells in bodily fluids, especially in low frequency, has long been a challenge in clinical medicine. Classic microscopy-based analysis, although the gold standard in diagnostics, lacks the throughput to consistently identify rare cell populations with confidence. Flow cytometry initially offered great promise, as acquisition rates were sufficiently high to provide significant numbers of events, but this approach depends largely on the availability of fluorescently-labeled markers to discriminate normal from neoplastic cells and ‘tumor specific’ markers have generally not been identified. Thus, the use of this antibody-based approach depends on ectopic expression of a normal antigenic epitope, formation of a new epitope through genetic mutation or recombination, or consistent modulation of the expression of a marker expressed in both transformed and non-transformed cells. The approach is further confounded by the diversity of neoplastic transformations and genetic heterogeneity in the human population.[13-15]

In contrast to single or multi-parameter antibody-based techniques, cellular morphology analysis is an effective means of cancer screening. For instance, dysplastic and neoplastic cells have been detected in lung sputum on the basis of morphology.[16] Likewise, exfoliated cells collected from bladder washings of bladder cancer patients have been shown to have distinct morphological and genetic changes.[17] Dysplastic morphology is also the primary diagnostic criterion in Pap smears, where microscope-based automated morphological analysis has been shown to be effective and approved by the FDA for primary screening.[18, 19]

In certain applications, such as the detection of carcinoma cells in the blood using a test commercialized by Immunicon Corporation (Huntingdon Valley, PA), the unique biochemical and morphological characteristics of the target cells offers a tremendous advantage. In this case, a combination of enrichment using a marker specific to epithelial cells (e.g., the epithelial cell adhesion molecule) followed by morphologic analysis has been shown to be effective at detecting rare cells in some metastatic cancer patients.[20] However, approximately two-thirds

of patients with metastatic carcinomas had either none or only one detectable carcinoma cell per 7.5 ml of blood, which is below the current threshold of five circulating tumor cells necessary to make a statistically robust diagnosis.[21, 22] Aside from the special case of tumor cell detection in the blood, a major issue in cancer detection is that the pathological cells may be present in the context of a large number of normal cells of the same type, leading to extended analysis times due to the relatively slow imaging and analysis rate of current imaging instrumentation and software.

The ImageStream system offers significant potential to enhance diagnostic capabilities by combining antibody based evaluation of expressed tumor-associated markers with morphological analysis in a single technology platform. In order to generate proof of principle data for the discrimination of neoplastic and normal epithelial cells using flow imagery, a mixture of both normal mammary epithelial and mammary carcinoma cells were imaged and analyzed. Mammary epithelial carcinoma cells were procured as frozen stocks from the American Type Tissue Culture Collection (ATCC, Manassas, VA). In order to better control for tumor-to-tumor variability, three different mammary epithelial carcinoma cell lines derived from different patients (HCC-1500, HCC-1569, and HCC-1428) were pooled at equal concentration for the study. The cell lines grew adherent to plastic and were expanded by routine tissue culture methods. Normal mammary epithelial cells were obtained from Cambrex Biosciences (Walkersville, MD) and expanded as recommended.

Normal and neoplastic mammary epithelial cells were harvested separately by brief incubation with trypsin/EDTA at 37° C. The cells were washed once in cold PBS containing 1% FCS, counted, and used experimentally. Normal mammary epithelial cells were stained with a fluorescein-conjugated monoclonal antibody to Class I HLA by incubating the cells with the appropriate, pre-determined dilution of the mAb for 30 minutes at 4° C. The labeling of normal mammary epithelial cells with anti-Class I MHC mAb allowed the normal cells to be identified in mixes of normal and carcinoma cells, thereby providing an objective “truth” to facilitate the identification of image features that distinguish normal epithelial cells from carcinoma cells. Mammary carcinomas are known to down-regulate Class I MHC expression but, as a precaution against passive transfer of antibody to the carcinoma cells, both the normal and pooled carcinoma cells were separately fixed in 1% paraformaldehyde prior to mixing. DRAQ5, a DNA binding dye that can be excited with a 488 nm laser and emits in the red (BioStatus, Ltd, Leicestershire, UK), was added to the sample prior to running on the ImageStream, providing DNA content and nuclear morphology features for the analysis.

After performing spectral compensation on the data file, an initial visual inspection was performed to compare normal mammary epithelial cells (positive for Class I HLA) to the unstained carcinoma cells. Representative images of normal cells are shown in Figure 1, and representative carcinoma cells are shown in Figure 2. Both Figures present each cell as a row of pseudocolored images in 6 channels (left to right): Channel 1 - blue laser side scatter (darkfield), Channel 2 - blank, Channel 3 - green HLA-FITC fluorescence, Channel 4 - blank, Channel 5 – brightfield imagery, and Channel 6 - red nuclear fluorescence.

Qualitative observations provided a starting point for the identification of quantitative features that distinguished the two populations. Normal cells were noted to have higher scatter intensity and heterogeneity, were generally larger, and had lower nuclear intensity. The subsequent analysis sought to quantitate these differences, as well as to discover additional parameters that might have discrimination power. A screen-capture of the IDEAS analysis of multiple discriminating parameters is shown in Figure 3.

The analysis shown in Figure 3 proceeded from the dot plot in the upper left of the Figure. Single cells were first identified based on a dot plot of brightfield area versus aspect ratio. A

gate was drawn around the population containing putative single cells based on the criteria of the area being large enough to exclude debris and the aspect ratio being greater than ~0.5, which eliminates doublets and clusters. The veracity of the gating was tested by examining random cells both within and outside of the gate using the software's "virtual cell sort" functionality that allows the visual inspection of individual cells by clicking on individual dots in the plot, and be presenting cell image galleries corresponding only to those cells that fall within a specific gated region.

Next, the normal mammary cells were distinguished from the mammary carcinoma cells using the anti-HLA Class I mAb that was applied only to the normal cells. The solid yellow histogram of FITC intensity was generated and is shown to the right of the dot plot. The FITC positive (normal mammary epithelial cells) and FITC negative (mammary epithelial carcinoma cells) were then gated as shown on the plot, resulting in populations of 2031 normal cells and 611 carcinoma cells. These populations were then used to identify features that quantitatively discriminated between normal and cancerous cells based on differential histograms.

The remaining 10 plots in Figure 3 are differential histograms of the normal cells (green populations) and carcinoma cells (red populations), with each plot representing a different quantitative feature. The 10 discriminating features fell into five distinct classes: scatter intensity, scatter texture, morphology, nuclear intensity, and nuclear texture.

Differential histograms 1-3 showed the difference between the two populations using three different, but correlated, scatter intensity features: "scatter mean intensity" (total intensity divided by cell area), "scatter intensity" (total intensity minus background), and "scatter spot small total" (total intensity of local scatter maxima). Although all three scatter intensity features provided good discrimination, "scatter mean intensity" was the most selective.

Differential histograms 4-5 quantitated scatter texture using either an intensity profile gradient metric ("scatter gradient RMS") or the variance of pixel intensities ("scatter frequency"), which proved more selective.

Differential histograms 6-8 plotted the cellular area (brightfield area), nuclear area (from the DNA fluorescence imagery), and cytoplasmic area (the difference of cellular and nuclear area). The carcinoma cell lines were generally smaller in brightfield area, confirming the qualitative observations from cell imagery. The nuclear area of the carcinoma cell lines was smaller than the normal cells, but to a degree proportional to the difference in cellular area, so the nuclear/cellular area ratio was not discriminatory. However, the cytoplasmic area was significantly lower in the carcinoma cells.

Finally, differential histograms 9 and 10 plotted the nuclear mean intensity and nuclear frequency (heterochromaticity), respectively. As in the case of scatter, both of these features provided some discriminatory power.

The multispectral/multimodal imagery collected by the ImageStream and analyzed using the IDEAS software package in this engineered experiment revealed a number of significant differences in darkfield characteristics, cellular morphology, DNA content, and nuclear morphology between normal epithelial and epithelial carcinoma cells. While it is well-recognized that cells adapted to tissue culture have undergone a selection process that may have altered their cellular characteristics, these data demonstrate that it is feasible to build an automated classifier that uses the morphometric and photometric features identified and described above to separate normal from transformed epithelial cells and possibly other cell types. The use of tumor-associated antibody based markers could possibly synergize with the morphological analysis to provide a greater depth of understanding of dysplastic changes and neoplastic transformations as well as a more accurate staging of these pathologies.

High Throughput Extended Depth of Field Imaging of Cells Subjected to *In Situ* Hybridization

Imaging flow cytometry is compatible with the broad range of cell staining protocols developed for conventional flow cytometry as well as those developed for imaging cells on slides, although with protocol modifications to the suspension format. Fluorescence *in situ* hybridization (FISH) is recognized as a slide-based imaging application which could benefit greatly by the greater throughput and quantitation of flow cytometry; and several groups have adapted hybridization techniques to cells in suspension.[23-26] However, the lack of spatial resolution in standard flow cytometry requires the substitution of total probe intensity for spot counting as a means of assessing results, thereby preventing the use of flow cytometry for the analysis of translocations, inversions, or other rearrangements. Though there are certain specific FISH applications that have strong and consistent signals, such as telomeric length analysis or the detection of the presence or absence of a Y chromosome, FISH probe intensity variation can be high and signal intensities often approach the detection limits of standard flow cytometry, reducing the reliability of aneuploidy assessment.[27-30]

Imaging flow cytometry is potentially well suited to FISH analysis because the detection limit of imaging flow cytometry improves as the size of the fluorescent signal source decreases.[31] Further, the quantitation of FISH-probed cells for applications such as aneuploidy analysis is accomplished by spot counting rather than relying exclusively on total intensity analysis, making it tolerant of wide variations in probe intensity and more consistent with the standard of practice in clinical FISH assessment.

To investigate the utility of imaging flow cytometry for clinical FISH analysis, human peripheral blood mononuclear cells (PBMC) were obtained (AllCells, San Diego, CA) and probed using a FISH in suspension (FISHIS®) protocol developed at Amnis Corporation. The cells were fixed and permeabilized with successive incubations in 30% (30 minutes at 4° C) then 70% (10 minutes at 4° C) Carnoy's solution (3:1 methanol: acetic acid) in PBS. After centrifugation, the cells were washed once in 2X SSC, then resuspended in hybridization buffer containing the SpectrumGreen labeled chromosome 12 enumeration probe according to the manufacturer's directions (Vysis, Des Plaines, IL). To hybridize the probe, cells in PCR tubes were exposed to 80° C for 5 minutes and 42° C for 2 hours in a DNA thermocycler. 100 ul of 2X SSC was added to the tubes and the cells pelleted by centrifugation. Cells were resuspended in 0.4X SSC containing 0.3% NP40 and exposed to 72° C for 2 minutes. The cells were centrifuged and the pellets were then resuspended in 50 ul of 1% paraformaldehyde (in PBS). The sample was then loaded into the ImageStream system and a file of 3,500 cells was collected.

Figure 4 is a gallery of 15 individual cells from the PBMC data file, numbered by the order in which they flowed through the instrument. Each cell is represented by a row of images (L-R): darkfield, chromosome 12 fluorescence, brightfield, and an overlay of the fluorescence and brightfield images. Doublets and larger clusters were eliminated from the analysis by plotting the area versus the aspect ratio of each cell's brightfield image on a dot plot and gating on single cells, which represented approximately 60% of the data and were clearly differentiated as a population having an aspect (length to width) ratio close to one and lower area than doublets and clusters. No other pre-selection was performed, so the gallery represents an unbiased sampling of FISH data in PBMC populations. Most cells had two well-resolved FISH spots, corresponding to the two copies of chromosome 12. However, a fraction of the cells had one or both FISH spots out of focus to some degree and/or only one apparent spot, corresponding to a cell orientation which superimposed the FISH spots from the perspective of the imaging system. Defocus is a problem that increases with cell size, while the frequency of FISH spot superposition would tend to decrease as cell size increases. The cells in the PBMC data file

were found to have a mean diameter of 6.4 +/−0.7 microns, which is relatively small compared to the nuclear size of many epithelial cell types.

To address the constraint that limited depth of field places on FISH analysis in larger cells assessed by imaging flow cytometry, a prototype ImageStream system having extended depth of field (EDF) image collection capabilities was developed.[32] The EDF version of the ImageStream system incorporates a specialized optical element in the standard optical system that causes light from widely different focal positions in the object to be imaged on the detector plane simultaneously in a process referred to as Wavefront Coding™ by its developer, CDM Optics, Inc. (Boulder, CO).[33] The modified imagery is post-processed to recover image sharpness while preserving the increased depth of focus that comes from the modification of the wavefront during data acquisition. Images acquired using the EDF version of the system have an effective depth of field of approximately 15 microns, resulting in a high resolution image of the cell with all features simultaneously in focus. Unlike confocal image stacking techniques, the Wavefront Coding methodology allows image acquisition at rates of hundreds of cells per second.

In order to compare FISH imagery between the standard and extended depth of field ImageStream configurations, Jurkat human lymphoma cells (ATCC) were grown in suspension culture, hybridized to a chromosome 8 probe (Vysis) using the FISHIS protocol described above, and imaged using both the EDF and standard ImageStream configurations. Figures 5 and 6 consist of galleries of standard and EDF images, respectively, of hybridized Jurkat cells classified as disomic for chromosome 8. In both galleries, each cell is represented by and overlay of its FISH spot fluorescence image (green) on its reduced-contrast brightfield image acquired at the same time. Because Jukats are known to exhibit cytogenetic instability, only single cells were included in each gallery based on their automated classification as having two chromosome 8 FISH spots, but no subjective selection criteria were employed in selecting the 25 images shown in each Figure. The degree of FISH spot focus enhancement with EDF imaging is qualitatively evident and improves the fidelity of automated spot analysis features (e.g., peak intensity, spot size, mean separation distance, etc.) by as much as ten-fold.[32]

Conclusion and Future Directions

Imaging flow cytometry is designed to marry the strengths of microscopy with those of flow cytometry, combining high resolution quantitative morphology and localization of fluorescent probes with sensitive multicolor phenotypic data from statistically meaningful populations of cells within minutes. The technology is commercially available for use in research and is being assessed for its clinical applicability. As demonstrated in the feasibility studies described here, the technique has the potential to greatly increase the clinician's ability to identify dysplastic and neoplastic cells obtained from bodily fluids. With the addition of extended depth of field capabilities, the technique may also greatly improve the precision and ac

References

1. Francastel C, Walters MC, Groudine M, Martin DI. A functional enhancer suppresses silencing of a transgene and prevents its localization close to centrometric heterochromatin. Cell Oct 29;1999 99(3): 259–269. [PubMed: 10555142]
2. Hulspas R, Bauman JG. The use of fluorescent in situ hybridization for the analysis of nuclear architecture by confocal microscopy. Cell Biol Int Rep Aug;1992 16(8):739–747. [PubMed: 1280185]
3. Orchard JA, Ibbotson RE, Davis Z, et al. ZAP-70 expression and prognosis in chronic lymphocytic leukaemia. Lancet Jan 10;2004 363(9403):105–111. [PubMed: 14726163]
4. Kay DB, Cambier JL, Wheeless LL Jr. Imaging in flow. J Histochem Cytochem Jan;1979 27(1):329–334. [PubMed: 374597]

5. Cambier JL, Kay DB, Wheeless LL Jr. A multidimensional slit-scan flow system. J Histochem Cytochem Jan;1979 27(1):321–324. [PubMed: 374595]
6. Basiji, DA.; Ortyn, WE. Imaging and analyzing parameters of small moving objects such as cells. Amnis Corporation, assignee. US patent 6211955. 2001. 2000-03-29
7. Basiji, DA.; Ortyn, WE. Imaging and analyzing parameters of small moving objects such as cells. Amnis Corporation, assignee. US patent 6249341. 2001. 2000-01-24
8. Pantel K, von Knebel Doeberitz M. Detection and clinical relevance of micrometastatic cancer cells. Curr Opin Oncol Jan;2000 12(1):95–101. [PubMed: 10687736]
9. Cancer Facts and Figures. Atlanta: American Cancer Society; 2004.
10. Ries, L.; Kosary, C.; Hankey, B.; Miller, B.; Edwards, B., editors. SEER Cancer Statistics Review 1973-1996. Bethesda: National Cancer Institute; 1999.
11. Dooley WC. The future prospect: ductoscopy-directed brushing and biopsy. Clin Lab Med Dec;2005 25(4):845–850. ix. [PubMed: 16308096]
12. Pantel K, Riethmuller G. Micrometastasis detection and treatment with monoclonal antibodies. Curr Top Microbiol Immunol 1996;213(Pt 3):1–18. [PubMed: 8814999]
13. Herlyn D, Herlyn M, Ross AH, Ernst C, Atkinson B, Koprowski H. Efficient selection of human tumor growth-inhibiting monoclonal antibodies. J Immunol Methods Oct 12;1984 73(1):157–167. [PubMed: 6491298]
14. Leitzel K, Lieu B, Curley E, et al. Detection of cancer cells in peripheral blood of breast cancer patients using reverse transcription-polymerase chain reaction for epidermal growth factor receptor. Clin Cancer Res Dec 1998;4(12):3037–3043.
15. Yuasa T, Yoshiki T, Tanaka T, Isono T, Okada Y. Detection of circulating testicular cancer cells in peripheral blood. Cancer Lett Aug 23;1999 143(1):57–62. [PubMed: 10465338]
16. Petty TL. The early identification of lung carcinoma by sputum cytology. Cancer Dec 1;2000 89:2461–2464. [PubMed: 11147627]
17. Halling KC, King W, Sokolova IA, et al. A comparison of cytology and fluorescence in situ hybridization for the detection of urothelial carcinoma. J Urol Nov;2000 164(5):1768–1775. [PubMed: 11025767]
18. Lee JS, Bannister WI, Kuan LC, Bartels PH, Nelson AC. A processing strategy for automated Papanicolaou smear screening. Anal Quant Cytol Histol Oct;1992 14(5):415–425. [PubMed: 1338567]
19. Patten SF Jr, Lee JS, Nelson AC. NeoPath, Inc. NeoPath AutoPap 300 Automatic Pap Screener System. Acta Cytol Jan-Feb;1996 40(1):45–52. [PubMed: 8604574]
20. Rao CG, Chianese D, Doyle GV, et al. Expression of epithelial cell adhesion molecule in carcinoma cells present in blood and primary and metastatic tumors. Int J Oncol Jul;2005 27(1):49–57. [PubMed: 15942643]
21. Tibbe AG, Miller MC, Terstappen LW. Statistical considerations for enumeration of circulating tumor cells. Cytometry A. Jan 2;2007
22. Allard WJ, Matera J, Miller MC, et al. Tumor cells circulate in the peripheral blood of all major carcinomas but not in healthy subjects or patients with nonmalignant diseases. Clin Cancer Res Oct 15;2004 10(20):6897–6904. [PubMed: 15501967]
23. Steinhaeuser U, Starke H, Nietzel A, et al. Suspension (S)-FISH, a new technique for interphase nuclei. J Histochem Cytochem Dec;2002 50(12):1697–1698. [PubMed: 12486094]
24. Trask B, van den Engh G, Pinkel D, et al. Fluorescence in situ hybridization to interphase cell nuclei in suspension allows flow cytometric analysis of chromosome content and microscopic analysis of nuclear organization. Hum Genet Mar;1988 78(3):251–259. [PubMed: 3162226]
25. Trask B, van den Engh G, Landegent J, in de Wal NJ, van der Ploeg M. Detection of DNA sequences in nuclei in suspension by in situ hybridization and dual beam flow cytometry. Science Dec 20;1985 230(4732):1401–1403. [PubMed: 2416058]
26. Bauman JG, van Dekken H. Flow cytometry of fluorescent in situ hybridization to detect specific RNA and DNA sequences. Acta Histochem Suppl 1989;37:65–69. [PubMed: 2475886]

27. Baumgartner A, Schmid TE, Maerz HK, Adler ID, Tarnok A, Nuesse M. Automated evaluation of frequencies of aneuploid sperm by laser-scanning cytometry (LSC). Cytometry Jun 1;2001 44(2): 156–160. [PubMed: 11378868]

28. Baerlocher GM, Mak J, Tien T, Lansdorp PM. Telomere length measurement by fluorescence in situ hybridization and flow cytometry: tips and pitfalls. Cytometry 2002;47(2):89–99. [PubMed: 11813198]

29. Rufer N, Dragowska W, Thornbury G, Roosnek E, Lansdorp PM. Telomere length dynamics in human lymphocyte subpopulations measured by flow cytometry. Nat Biotechnol 1998;16(8):743–747. [PubMed: 9702772]

30. Baerlocher GM, Lansdorp PM. Telomere length measurements in leukocyte subsets by automated multicolor flow-FISH. Cytometry A Sep;2003 55(1):1–6. [PubMed: 12938182]

31. Ortyn WE, Hall BE, George TC, et al. Sensitivity measurement and compensation in spectral imaging. Cytometry A Aug 1;2006 69(8):852–862. [PubMed: 16969805]

32. Ortyn WE, Perry DJ, Venkatachalam V, et al. Extended Depth of Field Imaging for High Speed Cell Analysis. Cytometry. in press

33. Cathey WT, Dowski ER. New paradigm for imaging systems. Appl Opt Oct 10;2002 41(29):6080–6092. [PubMed: 12389977]

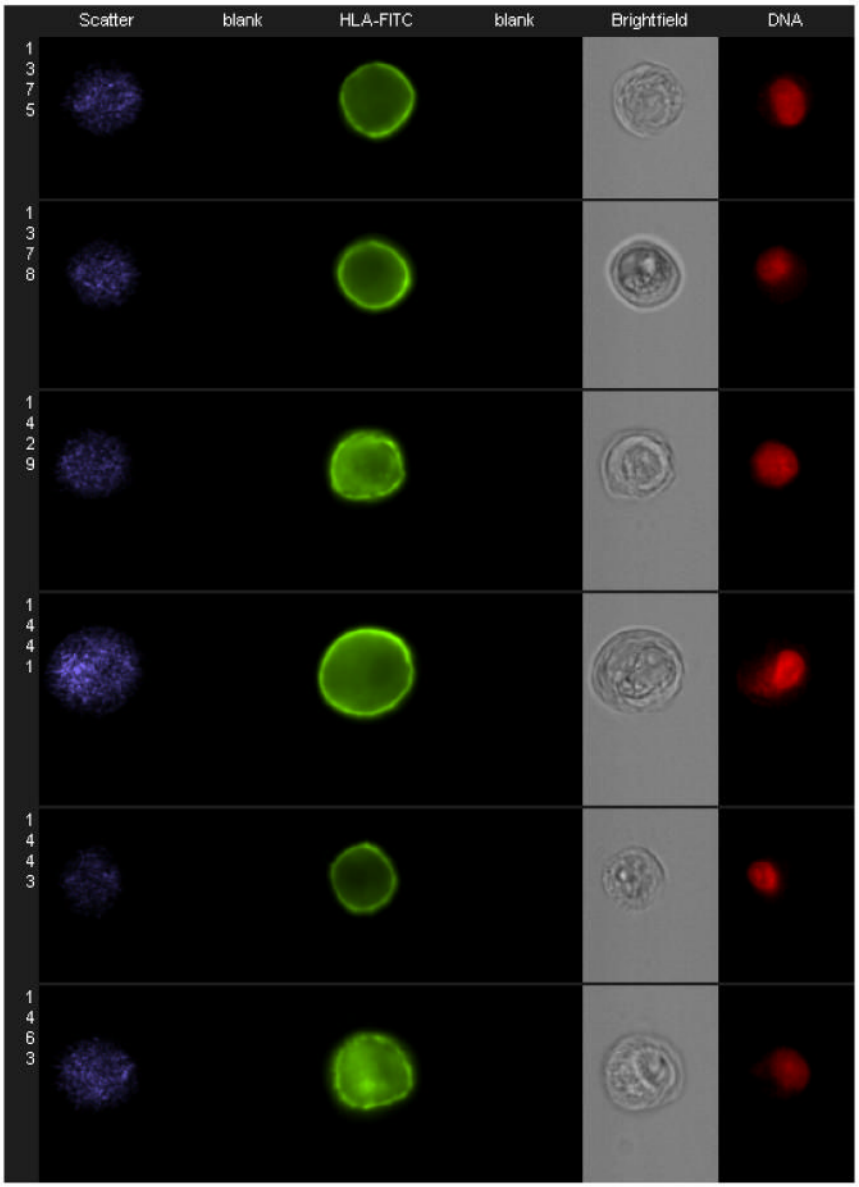

Figure 1.
Normal Mammary Epithelial Cells. Each cell is represented by a row of four images acquired simultaneously in flow, from left to right: darkfield (blue), FITC fluorescence from an HLA marker applied only to normal cells (green), brightfield (gray), and fluorescence from the DNA binding dye DRAQ5 (red).

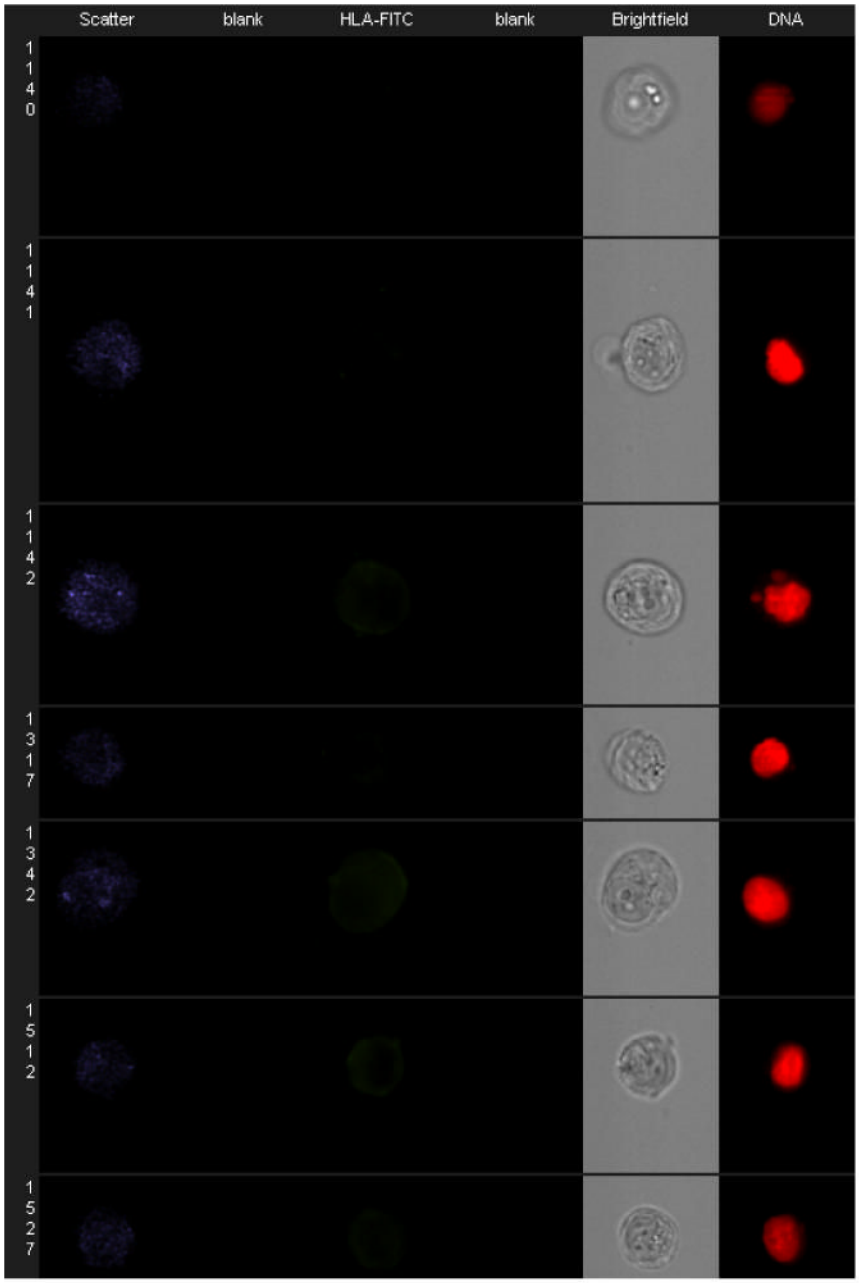

Figure 2.
Mammary Carcinoma Cells. Each cell is represented by a row of four images acquired simultaneously in flow, from left to right: darkfield (blue), FITC fluorescence (green), brightfield (gray), and fluorescence from the DNA binding dye DRAQ5 (red).

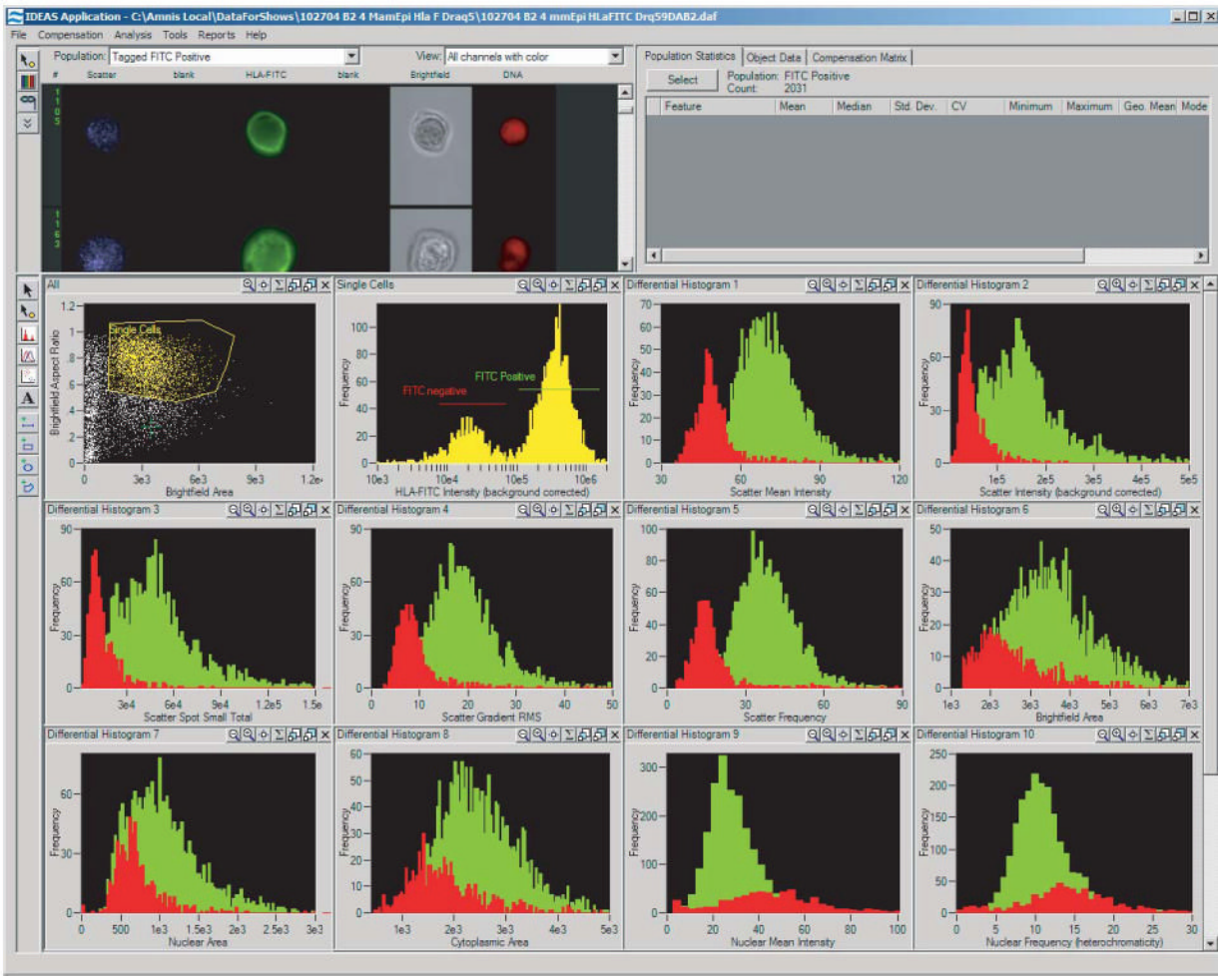

Figure 3.

Screen Capture of the IDEAS Statistical Image Analysis Package. Each of the 10 differential histograms represent a different quantitative parameter that discriminates between normal mammary cells (green distributions) and mammary carcinoma cells (red distributions) mixed in the same sample.

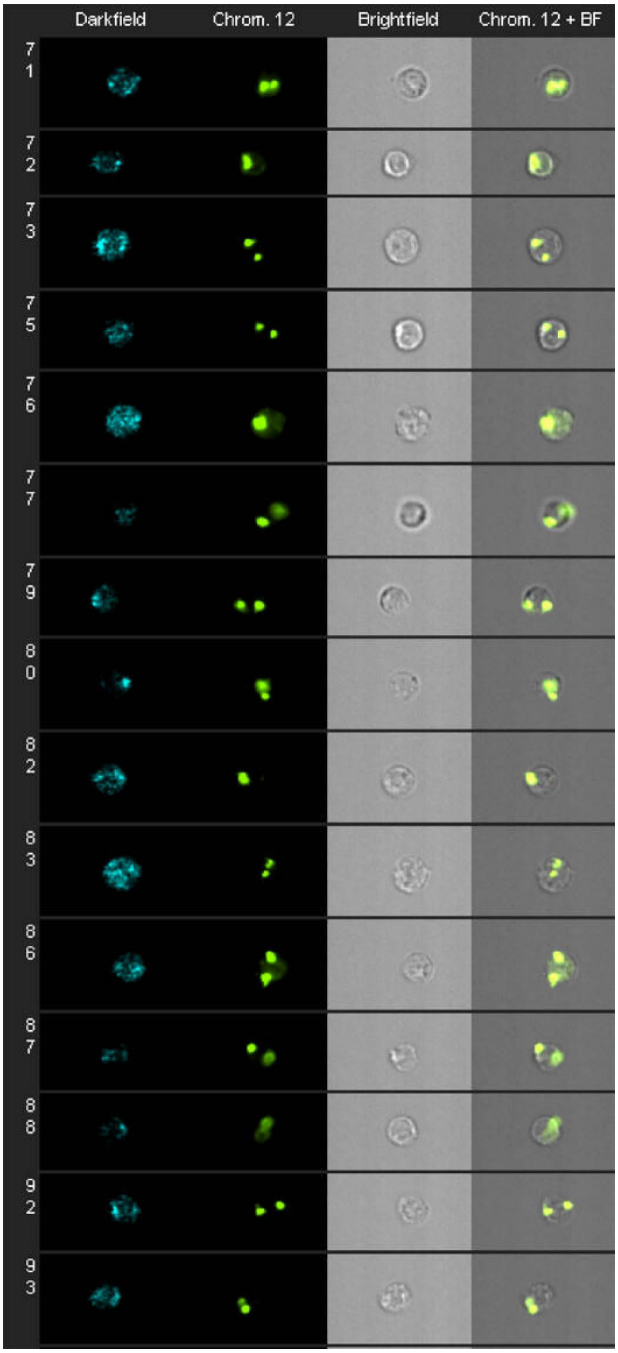

Figure 4.
Human Peripheral Blood Mononuclear Cells Hybridized in Suspension with a Chromosome 12 Probe. Each cell is represented by a row of four images, from left to right: darkfield (blue), fluorescence from a chromosome 12-SpectrumGreen probe (green), brightfield (gray), and a superposition of the fluorescence and brightfield images. An unbiased selection of cells illustrates variation in probe intensity, focus quality, and orientation with respect to the optic axis.

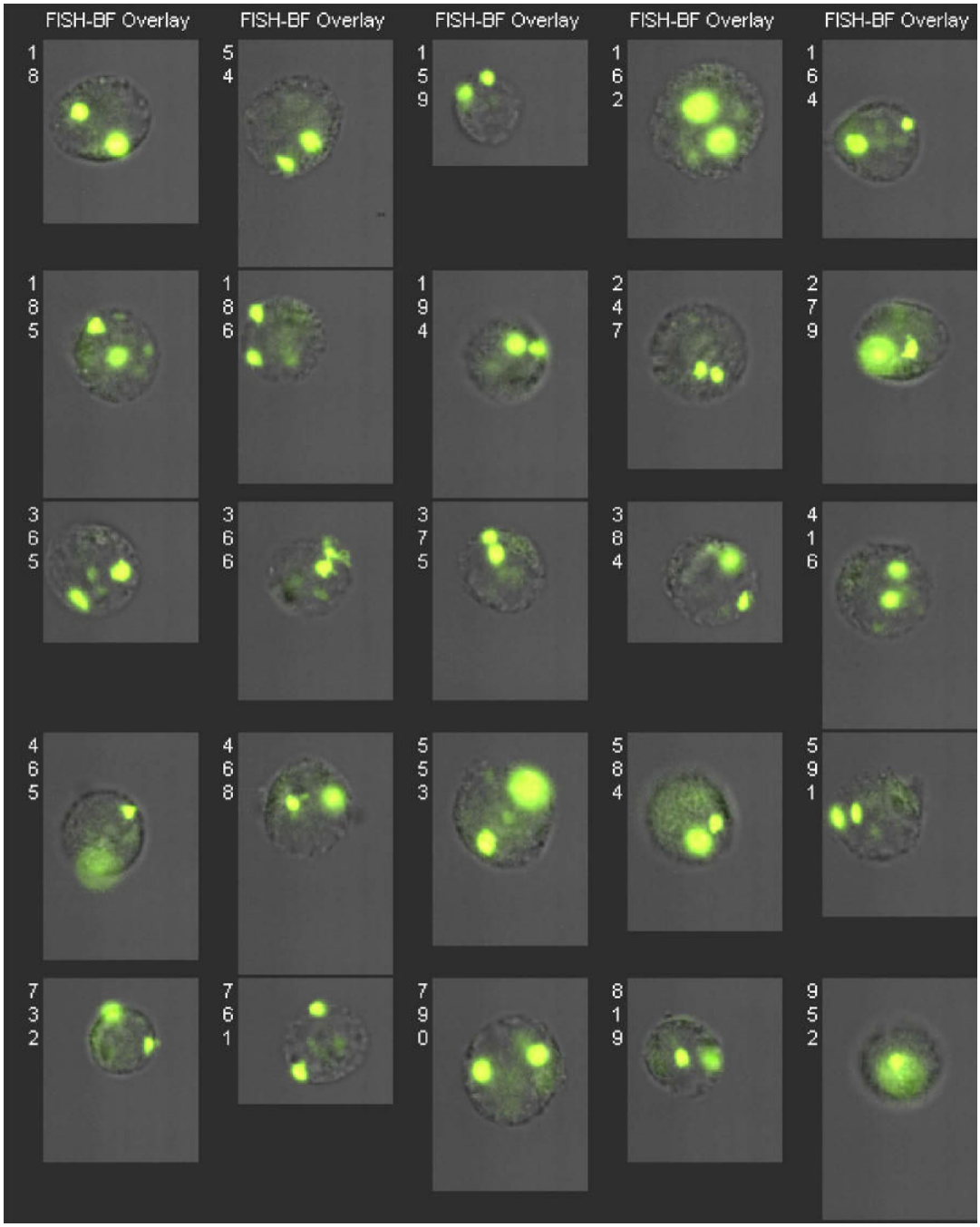

Figure 5.
Jurkat Cells Hybridized in Suspension with a Chromosome 8 Probe and Imaged in Flow Using Standard Optics. Each cell is represented by a superposition of its chromosome 8 fluorescence (green) and brightfield (gray) images. Jurkat cells are larger than human PBMC and exacerbate variations in image focus quality.

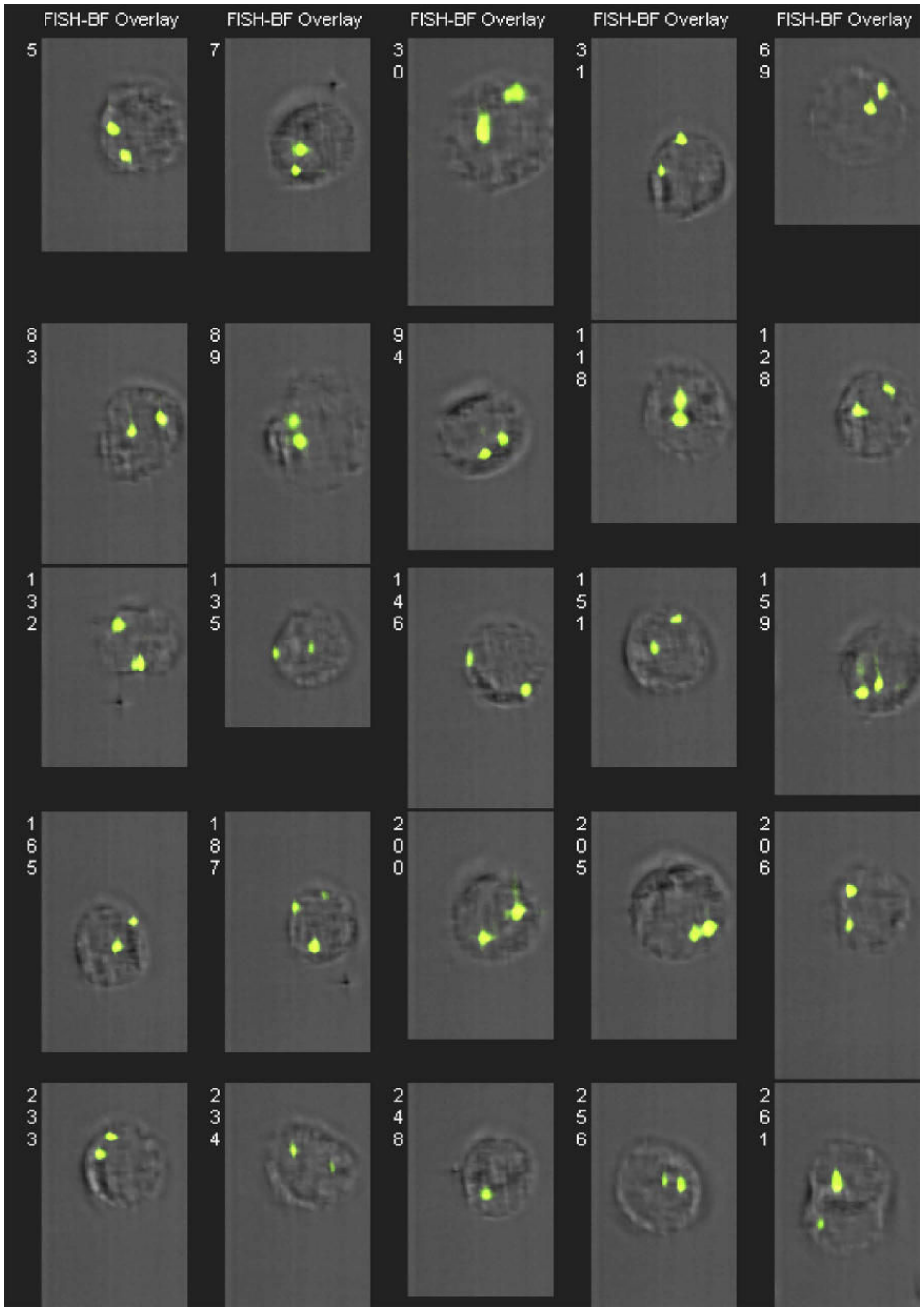

Figure 6.

Jurkat Cells Hybridized in Suspension with a Chromosome 8 Probe and Imaged in Flow Using Extended Depth of Field Optics. Each cell is represented by a superposition of its chromosome 8 fluorescence (green) and brightfield (gray) images. Extended depth of field imaging greatly improves focus quality and the accuracy of FISH spot enumeration.